

Low cost vision-based systems using smartphones for measuring deformation in structures for condition monitoring and asset management

R. Kromanis¹ and A. Al-Habaibeh².

¹Nottingham Trent University, Civil Engineering Department – UK, Email: rolands.kromanis@ntu.ac.uk

²Nottingham Trent University, Product Design Department – UK.

Abstract

Asset management is an important area in civil engineering. Monitoring deformations and movements of structures is an essential tool for the asset management and condition monitoring. Currently, a range of technologies such as contact (e.g. strain gauges and displacement sensors) and non-contact sensors (e.g. lasers, radars and cameras) is available for monitoring structural response. However, there is a need for low cost systems, which could be used for real life situations and laboratory environments (for teaching and research). This paper presents a novel approach of using smartphones to monitor movements in structures. The low-cost and easy to use hardware (i.e. smartphone) is readily available for the majority of people. The idea is that a smartphone camera is used to monitor specific markers (points of interest) on a structure. Movements of the markers can be obtained and calibrated for accurate movements of the structure. This paper presents results obtained from both lab structures and a full-scale bridge. Results show that the technology is a simple, low-cost and provides indicative and at the same time accurate information about structural response.

1. Introduction

Continuously aging civil infrastructure requires prudent, timely and accurate assessment. Asset maintenance costs are rising, especially for strategically and economically important assets such as bridges (Aktan et al., 1996). These assets have to provide an uninterrupted traffic flow, which plays a vital role in the modern society (Brownjohn, 2007). A large proportion of bridges have reached the end of their design life. Their maintenance costs are raising and their soundness is frequently questioned. The collapse of the I35W Bridge (Minneapolis, USA) in 2007 took lives of 13 people and injured 145 and daily economic loss was estimated to raise up to \$220,000 (Wald & Davey, 2008). The closure of the Forth Road Bridge (Edinburgh, UK) in late 2015 left a significant impact on economy in Scotland considering that a closure of a carriageway for one day can cost up to £650,000 (Hannan, 2015). Bridge collapses and closures could be if damages were detected early, which can be achieved with the aid of structural health monitoring (SHM) systems.

Currently, a range of SHM technologies such as contact sensors (e.g. strain gauges and linear variable differential transformer) and non-contact sensors (e.g. lasers and cameras) are available for condition monitoring of bridges. Installation of sensors can be a complicated process due to concerns related to access requirements. If contact sensors are chosen, an access to desired sensor locations is required. Access challenges can be avoided when considering non-contact measurement systems. Non-contact (or remote) measurement systems allow capturing structural changes without coming in a physical contact with the structure. A wide range of proprietary technologies such as spectral analysis, digital image correlation and radars (Vaghefi et al., 2012) are commonly deployed for the condition assessment of bridges and laboratory structures. However, there is a need for low-cost systems with potential applications in both real-life and lab (teaching and research) environments.

A number of researchers have investigated the advantages of vision-based strategies for monitoring structures (Ho, Lee, Park, & Lee, 2012; Lee, Fukuda, Shinozuka, Cho, & Yun, 2007; Lee & Shinozuka, 2006; Zaurin & Necati Catbas, 2010). Vision-based monitoring systems typically consist of cameras, which capture digital images of a structure (or part of it), and software, which analyses

images using image processing techniques. Methods, which can be employed to quantify displacements in bridges using image processing, have been validated on lab and full-scale structures (Lee et al., 2007), however low-cost (or freeware) tools for deformation monitoring are not commonly made available.

Vision-based systems can also indicate the location, number and types of vehicles on a bridge. This information can be coupled with measurements of structural response for damage detection (Zaurin & Catbas, 2010). Vision-based techniques can also be used to capture effects of ambient conditions, and, in particular, those due to temperature variations (Kromanis, 2015). At present, vision-based technologies are mainly deployed for short-term monitoring. Applications to long-term monitoring of bridges are still under development. Vision-based technologies hold a vast potential and may constitute a holistic monitoring system that can track vehicular traffic (Coifman, Beymer, McLauchlan, & Malik, 1998; Koller, Weber, & Malik, 1994; Liu & You, 2007), thermal loads (Kromanis, 2015) and human activities (Zhao & Chellappa, 2003), and also measure structural response.

This research investigates the capability of a low-cost vision-based system using a standard smartphone camera to measure structural deformations. A smartphone (Lenovo A806) is employed to capture images (and record videos) of structures under loadings. Collected visual information is then analysed using Matlab image processing toolbox (Mathworks, 2017). The performance of the proposed system has been investigated on laboratory structures and a full-scale bridge. Results show that structural deformations can be measured at required accuracies using the proposed system.

2. Methodology

All structures deform when subjected to loadings. Deformations of simple structures such as beams can be calculated using well-known engineering formulae. For example, a vertical deflection (δ) at any point of the length (l) of a cantilever beam, which is subjected to a point load (P) at its free end, can be calculated using the following equation:

$$\delta = \frac{Px^2}{6EI} (3l - x) \quad (1)$$

where x is the distance from the support at which δ is calculated, E is Young's modulus of the material and I is the second moment of area of the beam. For a rectangular beam with a known breadth (b) and height (h) I is calculated as follows:

$$I = \frac{bh^3}{12} \quad (2)$$

Eq. 1 shows that the deflection of a beam is directly related to P , E and I values. When considering a cantilever beam (with known E and I values) subjected to a point load at the free end, its deflection (δ) should be directly related to the applied load (P). However, if current δ is larger than previously observed δ when the beam is subject to the same P , a change in E and/or I values has occurred. For the above example, it is unlikely that E value would change leading to a conclusion that I value has changed, and the beam is damaged. In previous studies damage is introduced by making a cut in the beam (Farrar & Jauregui, 1998; Kim, Park, & Lee, 2007). When considering a rectangular beam, a cut in the top or bottom part of the section reduces the height of the beam, thus reducing I value.

A schematic representation of a vision-based system for measuring deformations such as vertical deflections in structures is provided in Figure 1. A cantilever beam is considered as a structure under loadings. The beam has artificial or natural markers (or points of interest) on its surface. Their relative

location is tracked by the software, and structural deformations are estimated. A smartphone camera is used to capture images while the beam is under loadings. The images are processed with algorithms analysing the movement of markers. Deformations of the beam are computed for each image. The load-response knowledge may then be used to assess the condition of the beam, for example using Eq. 1. For more complex structures such as bridges, the proposed vision-based system could be employed to obtain measurements that are used for structural identification and condition assessment.

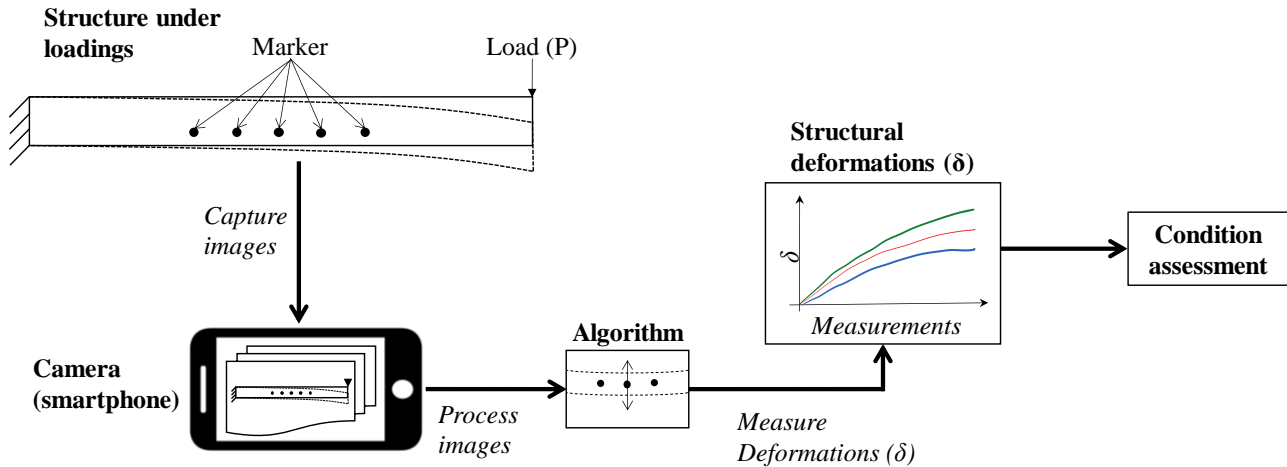


Figure 1 A schematic representation of condition assessment of a structure under loadings using a low cost vision-based measurement collection system with a smartphone camera.

3. Approach and technology

Vision-based technologies and image processing techniques have now been developed to an extent when they can enable fast and robust extraction of data from images. For example, video streams of traffic from a bridge can be combined with displacement measurements collected with contact sensors to create influence lines, which then serve as input features into damage detection methodologies (Zaurin & Catbas, 2010). For the successful application of the proposed vision-based system, algorithms, which focus solely on movements of selected markers, have to be developed. Processes involved when selecting markers on structures and analysing their movements are shown in the flow chart in Figure 2.

Once images of a structure under loadings are captured and saved/stored in a selected directory, information of structural movements can be obtained using image processing tools. Firstly, the reference image is selected. A desirable number of areas containing markers is set. A rectangle is used to draw a boundary identifying an area with a marker. These are then considered as separate images. Image adjustment parameters such as sharpness, intensity and number of pixels are altered to optimize the quality of the images with markers. Once the above processes are complete, an iterative process is initiated, in which images (starting from the first or selected image) are analysed in a consecutive order as follows:

- a) parameters for each image containing a marker are adjusted using adjustment parameters set for the reference images;
- b) background of the image is removed (only the marker is left in the image);
- c) the location of marker is calculated inputting a known measure;
- d) the pixel information is converted to a standardized measurement unit such as a millimetre;
- e) movement of the marker is saved for the i^{th} image.

The above process is repeated for all images of the structure under loadings. The movements of the selected markers are appended in a matrix forming time series of structural movements.

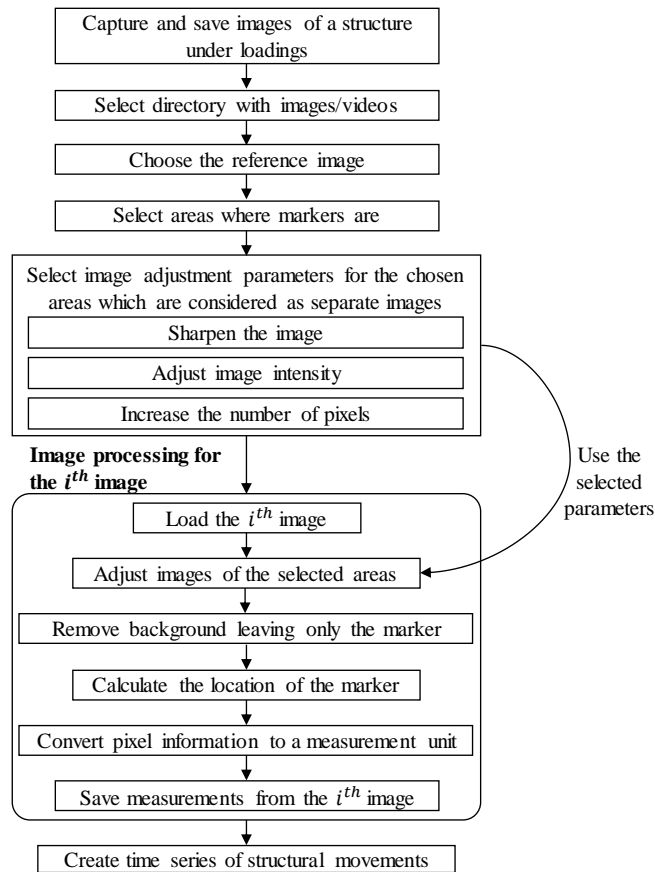


Figure 2 A flowchart of implemented processes in the proposed vision-based system.

3.1 Materials and patterns

Normally, each material has a unique texture and surface patterns. Some structural material such as aluminium and steel have uniform surface texture and may have no natural markers or patterns that can be used to track local deformations. However, the main focus of this study is on the development of the vision-base system for deformation monitoring using smartphones. For reasons of brevity, two structural materials (concrete and timber shown in Figure 3) with natural and artificial markers are discussed. Artificial markers are dots drawn with a marking pen. Natural markers are air voids in the concrete beam (Figure 3 (left)) and knots in the timber beam (Figure 3 (right)). Movements of markers can be obtained when estimating the location of markers in each image.

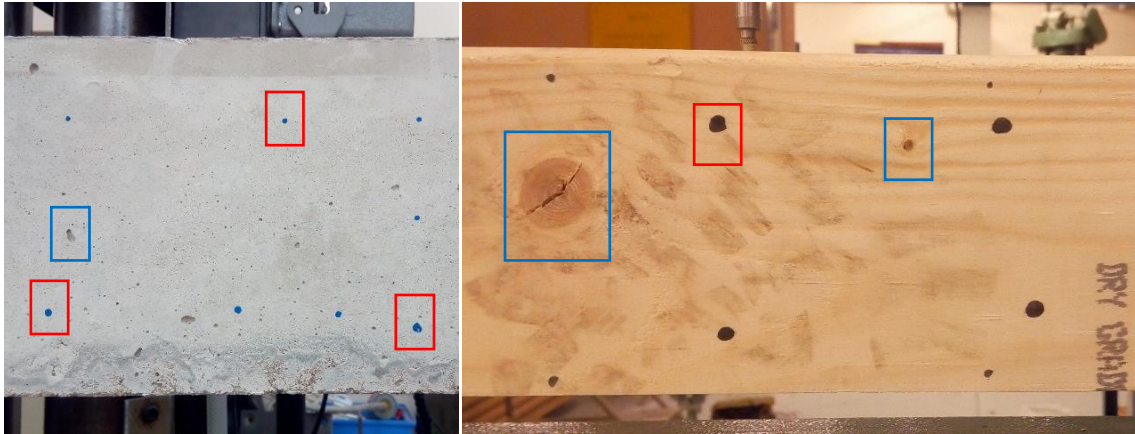


Figure 3 Concrete (left) and timber (right) beams with natural and artificial (created with a marking pen) markers or points of interest. Artificial and natural markers are shown in red and blue rectangles, respectively.

3.2 Application of image processing techniques

The general concept of digital image processing is to analyse an information content available in an image. For example, an image of a circle, which represents a marker on the beam, is captured using four resolution settings and shown in Figure 4. Figure shows that the quality of images depends on the set resolution of the camera. Higher resolution images offer more details than lower resolution images. Figure 4 shows images of the circle captured with low resolution cameras (a) 12 by 16 (12×16) pixels (px), (b) 12×16 px, (c) 24×32 px and with a high resolution camera (d) 768×1024 px.

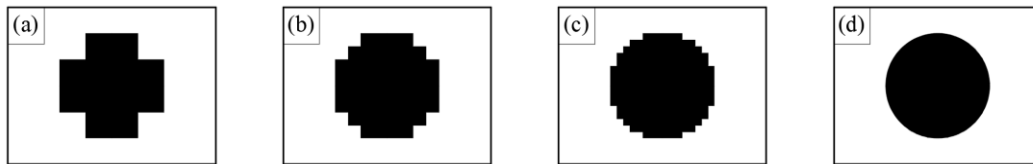


Figure 4 Images of a circle. The aspect ratio of the images is 4:3. The number of pixels in the images is as follow (a) 6×8 px, (b) 12×16 px, (c) 24×32 px and (d) 768×1024 px.

The movement of an object, say a circle shown in Figure 4, can be recognized when comparing the present image with the previous image. When multiple images are taken, while the object of interest moves, time series of object movements can be created. The resolution of an image plays an important role when estimating the movement of an object within the image. Pixel values are converted to standardised measurement units such as millimetres. The size of a pixel in millimetres (u_{px}) can be expressed using Eq. 3, in which a known distance (u) is divided by a number of pixels (N_p).

$$u_{px} = \frac{u}{N_p} \quad (3)$$

As an example, consider images (b1) and (c1) from Figure 5. The size of the frame of the image with a circle is 30 by 40 mm. From this information, the pixel size in vertical and horizontal directions can be calculated. The size of one pixel in the vertical and horizontal directions in image (b1) and image (c1) is $30/12 = 2.5 \text{ mm}$ and $30/24 = 1.25 \text{ mm}$, respectively. In images (b2) and (c2) the object has moved 1.25 mm down and to the right. However, this movement can only be detected in image (c2), which has higher resolution than image (b2). In images (b3) and (c3) the object has moved 2.5 mm down and to the right. This movement is recognized in both images.

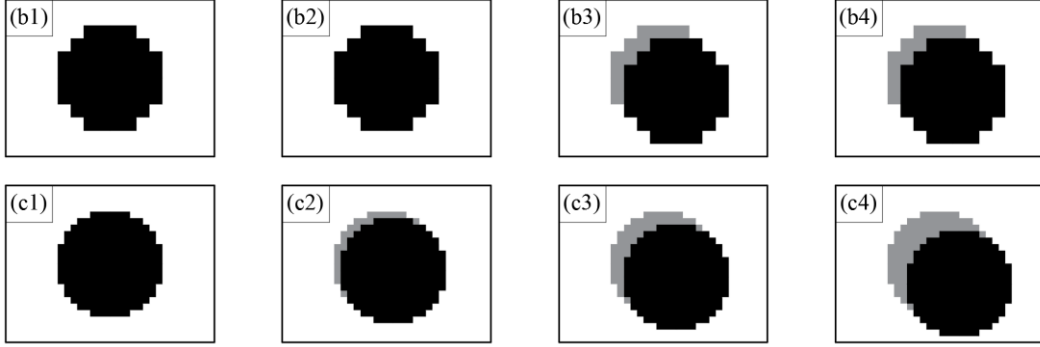


Figure 5 Movement of a circle in 12×16 px (b1, b2, b3, b4 (top)) and 24×32 px (c1, c2, c3, c4 (bottom)) images. The algorithmic steps employed in image processing in this study is shown in Figure 6. Initially an area with a marker (point of interest) is selected in the reference photo. In this example the reference photo is chosen to be a concrete beam shown in Figure 3 (left). The selected area with the marker (Figure 6 (a)) is taken from the bottom left part of the beam. A rectangle is drawn around the area containing a marker. The area should be large enough to cover the range of possible movements of the marker. The colour image of the area is converted to a grayscale image (Figure 6 (b)), therefore reducing the size of the information contained in the image and time required to analyse the image. Next, the sharpness and contrast of the grayscale image is adjusted (Figure 6 (c)). Then the adjusted image is converted to a binary (black and white) image. In these steps, an operator has to decide which parameters have to be altered to obtain the required quality of the image. In order to increase measurement precision, the number of pixels in the binary image are increased (Figure 6 (d)). For the given example, the scale of the image is increased four times. In the next step, connected pixels (components) are found. In Figure 6 (d) these are black dots, which are air voids in the concrete and the marker. Only the largest of the recognized components (the marker) is retained for further image analysis (Figure 6 (e)). Now, when only the marker is left in the image, its relative location can be calculated. The previous location of the marker can be compared with the present location of the marker, and its movement can be computed (Figure 6 (f))

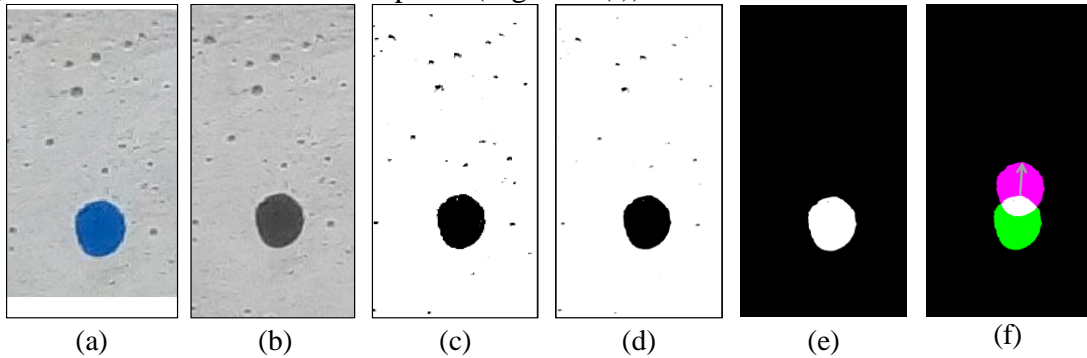


Figure 6 Steps involved in the image processing of an area with a marker. The selected area with a marker (a) is converted to a grayscale image (b) and then to a binary image (c). The number of pixels are increased (d), unnecessary markers are removed (e) and the movement of the marker can be tracked (f). Datasets of each i^{th} binary image, which are extracted from photos taken of the structure under loadings, are analysed as matrices.

$$\mathbf{U} = \begin{bmatrix} y_{11} & \cdots & y_{1n} \\ \vdots & \ddots & \vdots \\ y_{p1} & \cdots & y_{pn} \end{bmatrix} \quad (4)$$

y is a binary value (0 or 1) for a pixel in p by n matrix \mathbf{U} , where p and n is a row and column, respectively. When calculating the vertical location of the marker (δ_i) for each i^{th} image, only relevant pixel information of the top part of the marker is considered. The following algorithm is use:

Input

- A binary matrix \mathbf{U} of the selected area with the marker for each image.

Output

- A time series of vertical movements of the marker (δ_M) for the selected monitoring period.

Algorithm:

For each image i_j

For $m = 1$ to n in \mathbf{U}

$N_a =$ the number of the first row p with a nonzero value, $N_a \neq 0$

if a nonzero value is not found, proceed to the next column and do not put a value in N_a

Next column n in \mathbf{U}

$k =$ the number of elements in N , $k \leq n$

$$\delta = \frac{1}{k} (\sum_{o=1}^k N_o)$$

$$\delta_M(i) = \delta$$

Next i_j

4. Results

Three examples are selected to demonstrate the application of the proposed vision-based system for measurement collection using smartphones. In this study Lenovo A806 was used to capture images and videos. Initially the system is evaluated on two laboratory set-ups (i) a simply supported concrete beam and (ii) cantilever timber beam. Beams are subjected to both mechanically and manually applied loadings. Then a 20X optical lens is attached to the smartphone to evaluate if the proposed system can be employed to measure displacements of a footbridge exposed to forced vibrations.

4.1 Laboratory structures

An illustration of the proposed vision-based system using a smartphone for deformation monitoring of a laboratory structure is shown in Figure 7. Markers are drawn on the face of the structure. A smartphone is fixed on a tripod at a preferred distance from the lab structure. Setting the correct distance, at which photos (or video) are taken, has a direct impact on the resolution of images and calculated structural deformations. Understanding of structures is required to provisionally estimate expected movement of the structure. Then a suitable distance where a smartphone should be placed can be chosen. The collected images are analysed using the proposed image processing approach and algorithms, and time series of estimated structural movements are created.

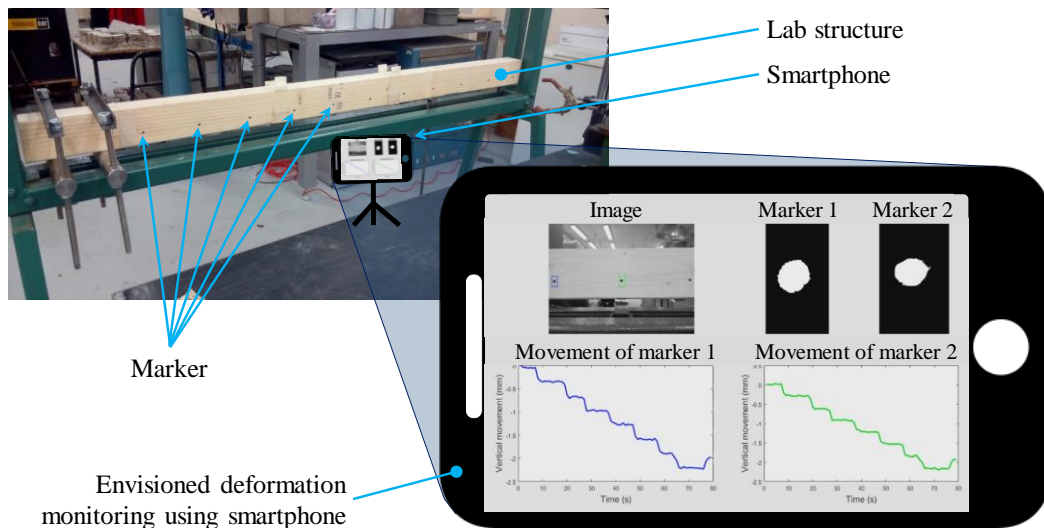


Figure 7 Envisioned set-up of the vision-based system using a smartphone for deformation monitoring of a beam in the structure's laboratory at Nottingham Trent University.

Concrete beam test

A simply supported concrete beam with the dimensions of 80 mm width, 130 mm height and 1200 mm length is subjected to three point flexural loadings. In the experimental set-up the supports are moving upward, therefore, vertical movements of the beam close to the right support are monitored. Markers are drawn on the surface of the beam. A smartphone is set 400 mm away from the beam. The camera is focused on the beam, and a 3120×4208 px image is taken once in two seconds. Two controlled loading scenarios are considered. The first loading scenario: at 140 s load is increased from 0 to 10 kN and kept for 50 s, then the load is increased to 14 kN and kept for 50 s before it is reduced to pre-load, which is around 4 to 6 kN. The second loading scenario: at 405 s load is increased from pre-load to 11 kN, kept for 20 s, increased to 12 kN, kept for 25 s, increased to 15 kN and kept for 25 s before it is removed (reduced to 0 kN). Four areas with markers are selected to analyse structural movements of the beam. The binary images of these areas are shown in Figure 8 (right). Time series of computed displacements of the markers are plotted in Figure 9. Displacement time series of the markers closely replicate the applied loading scenarios.

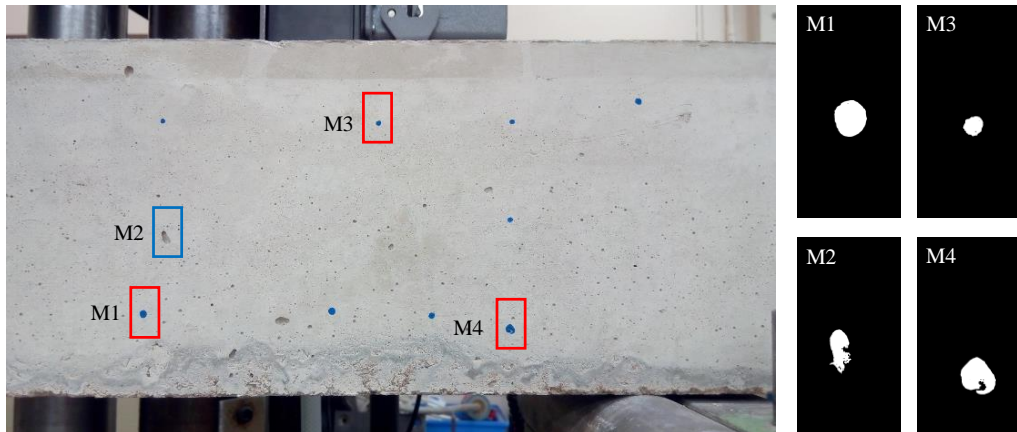


Figure 8 A part of the concrete beam under monitoring (left) and binary images of selected areas with markers (right). Red and blue rectangles on the photo of the concrete beam represent the selected areas with artificial and natural markers (M_i , where i is the number of a marker, $i = 1, 2, 3, 4$), respectively.

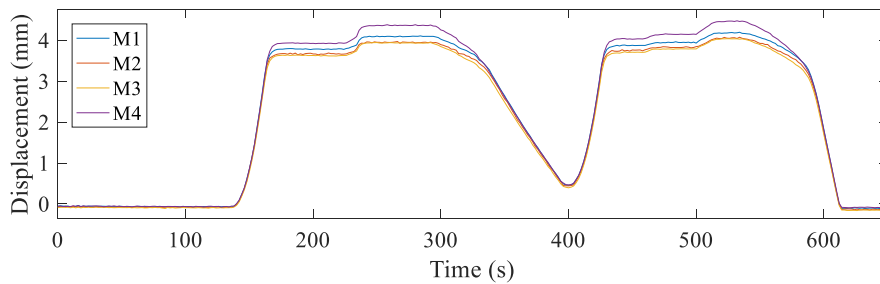


Figure 9 Time series of vertical movements of the selected markers on the concrete beam.

Timber cantilever test

The second laboratory set-up evaluates the performance of the proposed system on a timber cantilever beam with 120 mm height, 45 mm width and 1000 mm length. A hanger with a plate is attached to its free end to accommodate applied loadings. A smartphone is placed 400 mm away from the beam to capture deformations of the free end of the beam (see Figure 10 (right)) and focused. A 3072×4096 px image is taken once in three seconds. The load is applied manually using the following load steps: 0 N, 50 N, 100 N, 200 N, 300 N and 400 N. The load is removed as follows: 400 N, 300 N, 200 N, 100 N, 50 N and 0 N. This process describes one loading cycle. After the loading cycle has been repeated twice, a damage, in a form of a 27 mm cut in the top side of the beam close to its fixed end, is created. And the loading cycle is repeated.

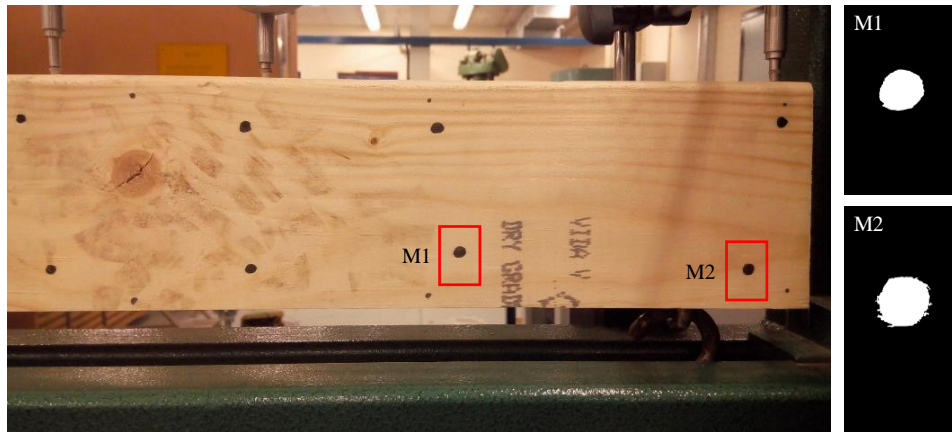


Figure 10 A part of the timber cantilever beam under monitoring (left). Red rectangles represent selected areas of artificial markers (M_i , where i is the number of a marker, $i = 1, 2$), which are analysed (right) using the proposed image processing approach.

Two areas with markers are selected (see Figure 10 (left)). Their binary images are shown in Figure 10 (right). Figure 11 shows time series of computed movements of the markers, which represents beam response to applied loadings. The load steps are clearly discernible in the plot. As anticipated, displacements of M2 are larger than those of M1, at similar loads. M2 is located further from the fixed end of the beam, therefore, according to Eq. 1, the vertical deflection at this location is expected to be the highest. Displacement time series are not as smooth as those computed for the concrete beam (see Figure 9). This can be related to the nature of applied loadings. The beam oscillates slightly when weights (in a form of steel plates) are applied. Noisy measurements between 750 s and 800 s, period when structure is being damaged, can be observed. After the onset of damaged, the magnitude of vertical deformations is larger than previously observed deformations (when structure was healthy). This indicates alteration in the cross section area of the beam (see Eq. 1 and Eq. 2) – damage.

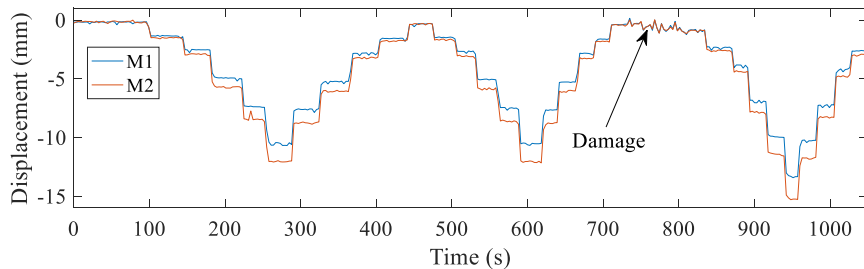


Figure 11 Time series of vertical movements of the selected markers on the timber beam.

4.2 Full-scale structure

The performance of the vision-based system is also evaluated on a full-scale bridge. The Wilford Bridge (see Figure 12) crosses the River Trent and is both a footbridge and aqueduct bridge. The bridge has a single 69 m long span. The smartphone is placed on a small tripod approximately 40 m away from the mid-span of the bridge, at which it is focused on. The bridge is excited by a group of people jumping at its mid-span. Videos are recorded while the bridge is exposed to forced vibrations. The frame size and collection rate of the videos are set to 1088×1920 px and 30 frames per second, respectively. While bridge response is collected, strong wind blows affecting the quality and collection of videos. While analysing some videos measurement noise is evident. For reasons of brevity, this is not shown in this study. A part of time series of bridge movements is shown in Figure 13. The first modal frequency can be extracted from time series. The modal frequencies is found to

be 1.688 Hz. This is very close to the model frequency obtained using Global Navigation Satellite System derived displacements by Psimoulis (2016), which is 1.7 Hz

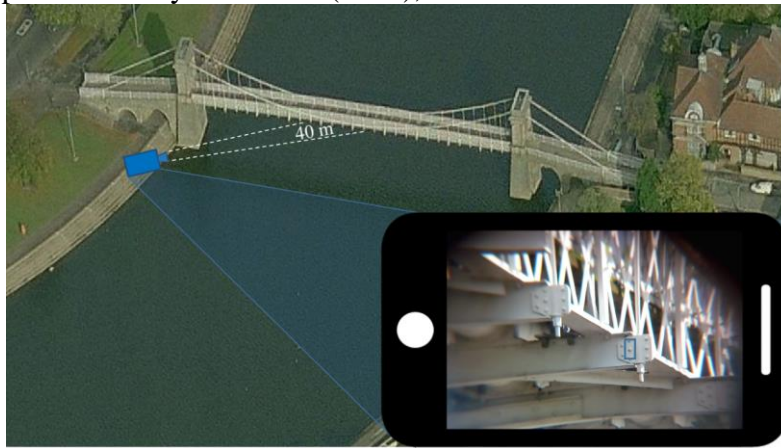


Figure 12 Monitoring of the Wilford bridge (Nottingham, UK) using the proposed vision-based system. Blue rectangle (in the image shown in the smartphone illustration) is the selected area with a natural marker (a head of the bolt).

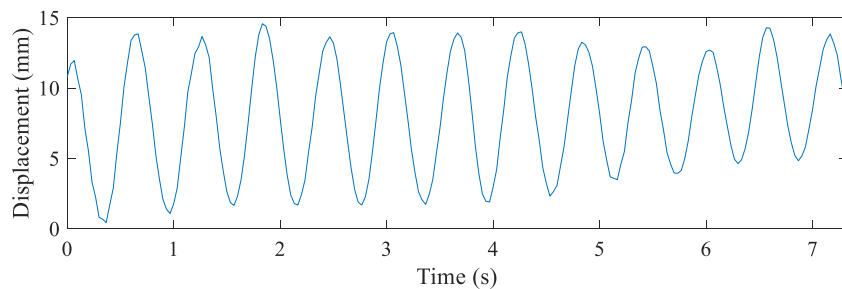


Figure 13 Time series of vertical movements measured at the mid-span of the bridge.

5. Conclusions

In structural health monitoring context the focus is on monitoring and analysing structural deformations. This study proposes a low cost vision-based system using smartphones for monitoring deformations. The premise is that the collected images or videos of the structure under loadings can be analysed to obtain structural deformations. The image processing approach is initiated with choosing a reference photo. Then areas with identified (or artificially created) markers (points of interest) on the structure are selected. A set of algorithms is employed to analyse the movement of these markers in subsequent images. This study draws the following conclusions:

- Indicative information of structural deformations can be obtained from collected images. Measurements obtained from the laboratory tests are within expected accuracies required for teaching and research. The accuracy is predominantly governed by the focus of the camera (image sharpness), distance from the structure under loadings, image resolution and the stability of the camera.
- Deformation monitoring of full-scale bridges could be made possible when adding an optical zoom lens to a smartphone. Results from the full-scale experiment show that sufficiently accurate deformations can be obtained to derive the first modal frequency of the bridge.

Low cost vision-based systems deploying smartphones for deformation monitoring have potential application in laboratory experiments. These systems could reduce costs of data acquisition systems and labour. The performance of proposed system has to be calibrated and compared with professional cameras and proprietary sensing systems (both contact and non-contact). It is anticipated that in near future smartphones will become faster and more powerful in their vision-based capacities than they

are now. Smartphones will allow taking high quality photos at high frequencies, therefore broadening SHM possibilities.

Acknowledgment

The authors would like to thank Dr Panagiotis Psimoulis and Dr Lukasz Bonenberg from the University of Nottingham for helping with measurement collection on the Wilford Bridge.

References

- Aktan, B. A. E., David, N. F., Vikram, L. B., Helmicki, A. J., Hunt, V. J., & Shelley, S. J. (1996). Condition assessment for bridge management. *Journal of Infrastructure Systems*, 2(3), 108–117.
- Brownjohn, J. M. W. (2007). Structural health monitoring of civil infrastructure. *Philosophical Transactions of the Royal Society a-Mathematical Physical and Engineering Sciences*, 589–622. <https://doi.org/DOI.10.1098/rsta.2006.1925>
- Coifman, B., Beymer, D., McLauchlan, P., & Malik, J. (1998). A real-time computer vision system for vehicle tracking and traffic surveillance. *Transportation Research Part C: Emerging Technologies*, 6, 271–288. Retrieved from <http://www.sciencedirect.com/science/article/pii/S0968090X98000199>
- Farrar, C. R., & Jauregui, D. A. (1998). Comparative study of damage identification algorithms applied to a bridge: I. Experiment. *Smart Materials and Structures*, 7(5), 704.
- Hannan, M. (2015). Forth Road Bridge closure will have huge impact on Scottish economy. Retrieved January 26, 2016, from <http://www.thenational.scot/news/forth-road-bridge-closure-will-have-huge-impact-on-scottish-economy.10831>
- Ho, H. N., Lee, J. H., Park, Y. S., & Lee, J. J. (2012). A synchronized multipoint vision-based system for displacement measurement of civil infrastructures. *The Scientific World Journal*. <https://doi.org/10.1100/2012/519146>
- Kim, J. T., Park, J. H., & Lee, B. J. (2007). Vibration-based damage monitoring in model plate-girder bridges under uncertain temperature conditions. *Engineering Structures*, 29(7), 1354–1365. <https://doi.org/10.1016/j.engstruct.2006.07.024>
- Koller, D., Weber, J., & Malik, J. (1994). *Robust multiple car tracking with occlusion reasoning*. Springer Berlin Heidelberg. Retrieved from http://link.springer.com/chapter/10.1007/3-540-57956-7_22
- Kromanis, R. (2015). *Structural Performance Evaluation of Bridges : Characterizing and Integrating Thermal Response*. University of Exeter.
- Lee, J. J., Fukuda, Y., Shinozuka, M., Cho, S., & Yun, C. (2007). Development and application of a vision-based displacement measurement system for structural health monitoring of civil structures. *Smart Structures and Systems*, 3(3), 373–384.
- Lee, J. J., & Shinozuka, M. (2006). A vision-based system for remote sensing of bridge displacement. *NDT & E International*, 39(5), 425–431. <https://doi.org/10.1016/j.ndteint.2005.12.003>
- Liu, Z., & You, Z. (2007). A Real-time Vision-based Vehicle Tracking and Traffic Surveillance. In *Eighth ACIS International Conference on Software Engineering, Artificial Intelligence, Networking, and Parallel/Distributed Computing (SNPD 2007)* (pp. 174–179). Ieee. <https://doi.org/10.1109/SNPD.2007.56>
- Mathworks. (2017). MATLAB image processing toolbox.
- Psimoulis, P. A., Peppas, I., Bonenberg, L., Ince, S., & Meng, X. (2016). Combination of GPS and RTS measurements for the monitoring of semi-static and dynamic motion of pedestrian bridge . In *In: 3rd Joint International Symposium on Deformation Monitoring (JISDM), 30 March - 1 April 2016, Vienna, Austria*.
- Vaghefi, K., Oats, R. C., Harris, D. K., Ahlborn, T. (Tess) M., Brooks, C. N., Endsley, K. A., ... Dobson, R. (2012). Evaluation of commercially available remote sensors for highway bridge condition assessment. *Journal of Bridge Engineering*, 17(6), 886–895.
- Wald, M. L., & Davey, M. (2008, January 16). States Advised to Check for a Bridge Design Flaw. *New York Times*, p. A17. Retrieved from http://www.nytimes.com/2008/01/16/washington/16bridge.html?_r=0
- Zaurin, R., & Catbas, F. N. (2010). Integration of computer imaging and sensor data for structural health monitoring of bridges. *Smart Materials and Structures*, 19(1), 15019. <https://doi.org/10.1088/0964-1726/19/1/015019>
- Zaurin, R., & Necati Catbas, F. (2010). Structural health monitoring using video stream, influence lines, and statistical analysis. *Structural Health Monitoring*, 10(3), 309–332. <https://doi.org/10.1177/1475921710373290>
- Zhao, W., & Chellappa, R. (2003). Face recognition: A literature survey. *Acm Computing Surveys (ACSU)*, 35(4), 399–458. Retrieved from <http://dl.acm.org/citation.cfm?id=954342>